Theory of exciton fine structure in semiconductor quantum dots : Quantum dot anisotropy and lateral electric field

Kadantsev, Eugene; Hawrylak, Pawel

Publisher's version / Version de l'éditeur:
https://doi.org/10.1103/PhysRevB.81.045311
Physical Review. B, Condensed Matter and Materials Physics, 81, 4, pp. 045311-1-045311-10, 2010-01-13

Theory of exciton fine structure in semiconductor quantum dots: Quantum dot anisotropy and lateral electric field

Eugene Kadantsev* and Pawel Hawrylak
Quantum Theory Group, Institute for Microstructural Sciences, National Research Council, Ottawa, Canada K1A 0R6
(Received 21 October 2009; revised manuscript received 14 December 2009; published 13 January 2010)

Theory of exciton fine structure in semiconductor quantum dots and its dependence on quantum-dot anisotropy and external lateral electric field is presented. The effective exciton Hamiltonian including long-range electron-hole exchange interaction is derived within the $k \cdot p$ effective-mass approximation. The exchange matrix elements of the Hamiltonian are expressed explicitly in terms of electron and hole envelope functions. The matrix element responsible for the "bright" exciton splitting is identified and analyzed. An excitonic fine structure for a model quantum dot with quasi-two-dimensional anisotropic harmonic oscillator confining potential is analyzed as a function of the shape anisotropy, size, and applied lateral electric field.

DOI: 10.1103/PhysRevB.81.045311 PACS number(s): 78.67.Hc, 73.21.La, 78.55.Cr

I. INTRODUCTION

One of the promising applications[1,2] of semiconductor quantum dots (QDs) (Refs. 3 and 4) for quantum cryptography is the generation of entangled photon pairs (EPPs) on demand.[5–8] EPPs can be generated with great efficiency via the biexciton cascade process (BCP) (Ref. 1) in which a biexciton radiatively decays into the ground state via two different indistinguishable paths involving two intermediate dipole-active (bright) exciton states. The major barrier to EPPs generation in BCP is the splitting of the intermediate "bright" exciton levels which distinguishes the paths of radiative decay and, as a result, destroys the entanglement. The splitting and mixing of the two bright exciton states is controlled by the long-ranged electron-hole exchange (LRE) interaction and depends on dot asymmetry and applied magnetic field.[6,8–10] Lateral electric fields have been applied in the hope to control the dot anisotropy and hence anisotropic exchange splitting.[11–13]

Better understanding of the electron-hole exchange interaction in QDs, particularly its LRE part, should help in the development of EPP generation schemes.

The exchange integral can be decomposed in real space into long-range part, i.e., exchange interaction between two "transition densities" localized in two different Wigner-Seitz (WS) cells and short-range part, i.e., exchange interaction within a single WS cell. A closely related decomposition of exchange into analytical and nonanalytical part exists in the reciprocal space. In what follows, we will use the "real space" definition of long-range and short-range exchange (SRE). We will reserve the use of words "local exchange" and "nonlocal exchange" to describe the type of integrals which contribute to the exchange matrix elements.

LRE electron-hole interaction in bulk semiconductors was investigated almost 40 years ago[14–16] and it is now well established that LRE splits the energy levels of bright excitons. For example, in zinc-blende direct band-gap semiconductors with fourfold-degenerate valence band Γ_{8v} and twofold-degenerate conduction band Γ_{6c}, the ground-state exciton is eightfold degenerate. The addition of SRE interaction into the excitonic Hamiltonian will split the eightfold-degenerate ground state into "dark" and bright multiplets with degeneracies of five and three. The addition of LRE interaction will further modify the fine structure by splitting threefold-degenerate bright exciton level into two transverse excitons with $J_z = \pm 1$ and one longitudinal exciton with $J_z = 0$.

Recent advances in single QD spectroscopies motivated reexamination of electron-hole exchange in systems with reduced dimensionality within the framework of envelope function approximation[17–23] and, more recently, from the point of view of atomistic empirical pseudopotential and tight-binding approximation.[24–28]

Within the envelope function approximation, Takagahara[17] have shown that if the electron-hole pair envelope contains only $Y_{00}(\theta, \phi)$ angular momentum component, then the long-range part of the electron-hole exchange vanishes. In Refs. 18 and 20, fine structure of localized exciton levels in quantum wells was considered. Efros *et al.*[19] and Gupalov *et al.*[22] investigated band-edge excitonic fine structure of spherical CdSe nanocrystals. In Ref. 21, Takagahara derived effective eight-band excitonic Hamiltonian which takes into account electron-hole exchange interaction. In particular, within the envelope function formalism of Refs. 17 and 21, LRE is a dipole-dipole interaction. Takagahara[21] applied his scheme to investigate excitonic fine structure of disklike GaAs/AlGaAs QDs as a function of QD anisotropy and size. It was demonstrated numerically in Ref. 21 that LRE vanishes for the ground-state bright exciton doublet in QDs with rotationally symmetric three-dimensional confining potential. A similar to that of Ref. 21 representation of the electron-hole exchange was discussed by Maialle *et al.*[18] in connection with the exciton spin dynamics in quantum wells.

Within atomistic empirical approach it has been demonstrated that the physical origin of long-range exchange interaction might be different from that of bulk[24] and that LRE has a nonvanishing magnitude even in "shape-symmetric" dots.[26,27] The former and the latter stem from the loss of local orthogonality on the unit-cell scale between electron and hole single-particle orbitals compared to the bulk case and "reduced" symmetry of the atomistic confining potential, respectively. For $\Gamma_6 \times \Gamma_7$ exciton, Gupalov *et al.*[25] identified the dipole-dipole and monopole-monopole contributions to the LRE with the intra-atomic and interatomic transition densities, respectively.

In this work, we will reexamine electron-hole exchange within the framework of envelope approximation. We note that Takagahara's condition[17] for the vanishing of LRE in spherically symmetric quantum dots constitutes only a *sufficient* condition for quenching of LRE. It does not explain, for example, why LRE vanishes in disklike QDs with rotational ($C_{\infty v}$) symmetry. These QDs are "squeezed" in one direction and the ground-state envelopes of single-particle states will contain angular momentum components that are higher than $Y_{00}(\theta,\phi)$. Motivated by recent experiments, we will investigate, within our model, the effects of the external electric field and size scaling of LRE interaction.

We derive here effective "four-band" excitonic Hamiltonian which includes effects of LRE interaction. The elements of the effective Hamiltonian are expressed explicitly in terms of envelope functions. The "microscopic parts" of single-particle orbitals are integrated out and enter the effective Hamiltonian as numerical parameters. The number of bands is truncated to two conduction and two valence bands for the simplicity of the interpretation. We present explicit expression for the matrix element responsible for the bright exciton splitting and, therefore, establish a new sufficient condition for LRE quenching.

An excitonic fine structure for a model system in which the confining potential has a form of two-dimensional-like anisotropic harmonic oscillator (2DLAHO) is considered as a function of lateral anisotropy. We present an explicit expression for the bright splitting of excitonic ground state as a function of lateral anisotropy. It is found, in agreement with previous work,[21] that, within the envelope approximation, the bright ground-state exciton splitting vanishes in the case of laterally isotropic confining potential. The quenching of bright exciton splitting coincides with vanishing of the matrix element responsible for the bright exciton splitting in our effective Hamiltonian.

We also analyze the effect of the lateral electric field on the excitonic fine structure of our model quantum dot. We find that the bright exciton splitting decreases due to the spatial separation of electron and hole envelopes.

Finally, the scaling of the bright exciton splittings with system's size is analyzed. It is found that the scaling of bright exciton splittings differ from the laws established using simple dimensionality arguments.

Effective units of length and energy are used throughout unless otherwise specified. The lengths are measured in effective Bohr's $a_{eB}=\epsilon\hbar^2/(m^*e^2)$, where ϵ is dielectric constant and m^* is the conduction-band effective mass. Energies are measured in effective Hartree's, 1 hartree $=m^*e^4/(\epsilon\hbar)^2=2$ Ry*. For example, using material parameters for GaAs, $a_{eB}=97.9$ Å and 1 hartree$=11.86$ meV.

II. THEORY OF EXCITON FINE STRUCTURE IN ENVELOPE FUNCTION APPROXIMATION

We now describe the single-particle states and the exciton fine structure in the envelope function approximation. The single-particle orbitals of the electron in a quantum dot are two-component spinors (two-row columns) written as

$$\phi(\mathbf{r})=\begin{pmatrix}\phi_a(\mathbf{r})\\ \phi_b(\mathbf{r})\end{pmatrix}=\phi_a(\mathbf{r})|\alpha\rangle+\phi_b(\mathbf{r})|\beta\rangle,$$

$$|\alpha\rangle=\begin{pmatrix}1\\0\end{pmatrix},\quad |\beta\rangle=\begin{pmatrix}0\\1\end{pmatrix}. \tag{1}$$

A dagger sign † will denote complex conjugation for complex quantities.

With $c^\dagger$ and $h^\dagger$ (c and h) electron and hole creation (annihilation) operators, the interacting electron-hole Hamiltonian can be written as

$$\hat{H}_X=\hat{H}_e+\hat{H}_h+\hat{H}_{int},\quad \hat{H}_e=\sum_i \varepsilon_i^e c_i^\dagger c_i,\quad \hat{H}_h=\sum_j \varepsilon_j^h h_j^\dagger h_j,$$

$$\hat{H}_{int}=\sum_{ijkl} c_i^\dagger h_j^\dagger h_k c_l\left(-\frac{1}{\epsilon}V^C_{ikjl}+V^E_{iklj}\right),$$

$$V_{ijkl}=V(i,j;k,l)=\int\int d\mathbf{r}_1 d\mathbf{r}_2 \frac{\phi_i^\dagger(\mathbf{r}_1)\phi_j^\dagger(\mathbf{r}_2)\phi_k(\mathbf{r}_2)\phi_l(\mathbf{r}_1)}{|\mathbf{r}_1-\mathbf{r}_2|}, \tag{2}$$

where $\hat{H}_e$, $\hat{H}_h$, and $\hat{H}_{int}$ are electron, hole, and electron-hole interaction Hamiltonian, respectively. The electron-hole interaction Hamiltonian consists of two parts: V^C/ϵ is the direct electron-hole Coulomb attraction screened by static dielectric constant ϵ and V^E is the electron-hole exchange interaction. The question of screening of electron-hole exchange is a subtle one and it is generally agreed that, at least, parts of the electron-hole exchange should be screened. In Ref. 29 (page 252), the long-range electron-hole exchange interaction in reciprocal space is screened by the high-frequency dielectric constant. We will assume, for now, that our exchange interaction V^E contains screening implicitly.

To obtain excitonic states, Hamiltonian (2) is diagonalized in the basis of all electron-hole pairs of the type $c^\dagger h^\dagger|g.s.\rangle$, where $|g.s.\rangle$ denotes a many-body state with fully occupied valence and empty conduction bands.

In this work, the hole and electron single-particle states are computed in the effective-mass approximation (EMA) (Refs. 29 and 30) which neglects band coupling in the single-particle states. In EMA, the hole ϕ_h and electron ϕ_e single-particle states are uniquely specified by band label (valence vj_z' and conduction $c\sigma'$) and envelop index (r and p), for example,

$$\phi_h(\mathbf{r})=F^r_{vj_z'}(\mathbf{r})u_{vj_z'}(\mathbf{r}),$$

$$\phi_e(\mathbf{r})=F^p_{c\sigma'}(\mathbf{r})u_{c\sigma'}(\mathbf{r}). \tag{3}$$

Here, $u(\mathbf{r})$ is the periodic part of Bloch eigenstate at $\mathbf{k}=0$. In what follows, $u(\mathbf{r})$ is a two-component spinor. We will assume that "bra" electron-hole pair is described by indices $c\sigma s$ and vj_zq, respectively.

The excitonic Hamiltonian matrix element in the basis of electron-hole pairs is

$$\langle g\,.\,s.|h_{vj_zq}c_{c\sigma s}\hat{H}_X c^{\dagger}_{c\sigma' p}h^{\dagger}_{vj'_zr}|g\,.\,s.\rangle$$
$$= \delta_{vj_zq,vj'_zr}\delta_{c\sigma s,c\sigma' p}(\varepsilon^h_{vj_zq}+\varepsilon^e_{c\sigma s})$$
$$- V^C(c\sigma s,vj'_zr;vj_zq,c\sigma' p)/\epsilon$$
$$+ V^E(c\sigma s,vj'_zr;c\sigma' p,vj_zq). \quad (4)$$

The effective Hamiltonian which involves only envelope functions is obtained by integrating out "microscopic" degrees of freedom (u). The derivation follows that of Ref. 21. Assuming T_d symmetry of the crystal, two conduction-band microscopic functions $|c1/2\rangle$ and $|c-1/2\rangle$ with spin projections $s_z=1/2$ and $s_z=-1/2$ are written as

$$u_{c1/2}(\mathbf{r}) = \langle \mathbf{r}|c1/2\rangle = \chi_s(r)\begin{pmatrix} Y_{00}(\hat{r}) \\ 0 \end{pmatrix},$$

$$u_{c-1/2}(\mathbf{r}) = \langle \mathbf{r}|c-1/2\rangle = \chi_s(r)\begin{pmatrix} 0 \\ Y_{00}(\hat{r}) \end{pmatrix}. \quad (5)$$

In Eq. (5), we assumed that microscopic conduction-band function are of pure s symmetry.

Two valence-band microscopic functions $|v-3/2\rangle$ and $|v+3/2\rangle$ with hole angular momentum projections $j_z=-3/2$ and $j_z=3/2$ are taken as

$$u_{v-3/2}(\mathbf{r}) = \langle \mathbf{r}|v-3/2\rangle = \chi_p(r)\begin{pmatrix} Y_{11}(\hat{r}) \\ 0 \end{pmatrix},$$

$$u_{v+3/2}(\mathbf{r}) = \langle \mathbf{r}|v+3/2\rangle = \chi_p(r)\begin{pmatrix} 0 \\ Y_{1-1}(\hat{r}) \end{pmatrix}. \quad (6)$$

In Eq. (6) we assumed that microscopic valence-band functions are of pure p symmetry. The eigenfunctions of angular momentum $\chi_p(r)Y_{11}(\hat{r})$ and $\chi_p(r)Y_{1-1}(\hat{r})$ can be expressed in terms of Cartesian functions p_x and p_y. We, therefore, are neglecting p_z contribution to the microscopic valence-band functions.

In what follows, we give a brief derivation of the effective excitonic Hamiltonian.

A. Calculation of Coulomb direct matrix elements

The unscreened Coulomb direct matrix element is given by

$$V^C(c\sigma s,vj'_zr;vj_zq,c\sigma' p) = \int\int d\mathbf{r}_1 d\mathbf{r}_2 \frac{q_1(\mathbf{r}_1)q_2(\mathbf{r}_2)}{|\mathbf{r}_1-\mathbf{r}_2|},$$

$$q_1(\mathbf{r}_1) = F^{s\dagger}_{c\sigma}(\mathbf{r}_1)u^{\dagger}_{c\sigma}(\mathbf{r}_1)F^{p}_{c\sigma'}(\mathbf{r}_1)u_{c\sigma'}(\mathbf{r}_1),$$

$$q_2(\mathbf{r}_2) = F^{r\dagger}_{vj'_z}(\mathbf{r}_2)u^{\dagger}_{vj'_z}(\mathbf{r}_2)F^{q}_{vj_z}(\mathbf{r}_2)u_{vj_z}(\mathbf{r}_2), \quad (7)$$

where we explicitly presented electron and hole single-particle orbitals as a product of an envelope F and a microscopic part u. The unscreened Coulomb attraction matrix element is just Coulomb interaction between two transition densities, where each "transition density" is a product of two electron orbitals or two valence orbitals. The matrix element is approximated as

$$V^C(c\sigma s,vj'_zr;vj_zq,c\sigma' p)$$
$$= \delta_{c\sigma c\sigma'}\delta_{vj_zvj'_z}\int\int d\mathbf{r}_1 d\mathbf{r}_2$$
$$\times \frac{F^{s\dagger}_{c\sigma}(\mathbf{r}_1)F^{p}_{c\sigma'}(\mathbf{r}_1)F^{r\dagger}_{v\sigma'}(\mathbf{r}_2)F^{q}_{v\sigma}(\mathbf{r}_2)}{|\mathbf{r}_1-\mathbf{r}_2|}. \quad (8)$$

B. Calculation of Coulomb exchange matrix elements

The exchange matrix element can be written as

$$V^E(c\sigma s,vj'_zr;c\sigma' p,vj_zq) = \int\int d\mathbf{r}_1 d\mathbf{r}_2 \frac{q_1(\mathbf{r}_1)q_2(\mathbf{r}_2)}{|\mathbf{r}_1-\mathbf{r}_2|},$$

$$q_1(\mathbf{r}_1) = F^{s\dagger}_{c\sigma}(\mathbf{r}_1)u^{\dagger}_{c\sigma}(\mathbf{r}_1)F^{q}_{vj_z}(\mathbf{r}_1)u_{vj_z}(\mathbf{r}_1),$$

$$q_2(\mathbf{r}_2) = F^{p}_{c\sigma'}(\mathbf{r}_2)u_{c\sigma'}(\mathbf{r}_2)F^{r\dagger}_{vj'_z}(\mathbf{r}_2)u^{\dagger}_{vj'_z}(\mathbf{r}_2). \quad (9)$$

The exchange matrix element can be thought of as a Coulomb interaction of two transition densities, where each transition density is a product of electron-hole single-particle orbitals.

We decompose exchange integral [Eq. (9)] into the short-range and long-range contributions in real space. We will refer to the whole integration region as Born-von Karmen cell (BvK cell) and to the individual unit cell within BvK cell as WS cell. The double integration over BvK cell (which consists of N_{cell} WS cells) is replaced by $N_{cell}\times N_{cell}$ integrals over WS cells,

$$\int_{\mathbf{r}_1\in \mathrm{BvK}}\int_{\mathbf{r}_2\in \mathrm{BvK}} d\mathbf{r}_1 d\mathbf{r}_2$$
$$\rightarrow \sum_{i=1}^{N_{cell}}\int_{\mathbf{r}_1\in \mathrm{WS}(\mathbf{R}_i)}\int_{\mathbf{r}_2\in \mathrm{WS}(\mathbf{R}_i)} d\mathbf{r}_1 d\mathbf{r}_2$$
$$+ \sum_{\substack{i,j=1 \\ i\neq j}}^{N_{cell}}\int_{\mathbf{r}_1\in \mathrm{WS}(\mathbf{R}_i)}\int_{\mathbf{r}_2\in \mathrm{WS}(\mathbf{R}_j)} d\mathbf{r}_1 d\mathbf{r}_2, \quad (10)$$

where $\mathbf{R}_i$ and $\mathbf{R}_j$ label positions of the WS cells. The first term in Eq. (10) consists of N_{cell} integrals in which $\mathbf{r}_1$ and $\mathbf{r}_2$ go over the same cell whereas the second term consists of $N_{cell}\times(N_{cell}-1)$ integrals in which $\mathbf{r}_1$ and $\mathbf{r}_2$ go over two distinct WS cells. The first sum in which $\mathbf{r}_1$ and $\mathbf{r}_2$ go over the same cell is the short-range exchange $V^{\mathrm{E}}_{\mathrm{SR}}$ whereas the second sum in which $\mathbf{r}_1$ and $\mathbf{r}_2$ go over two different WS cells is the long-range exchange $V^{\mathrm{E}}_{\mathrm{LR}}$.

The "effective" expression for the exchange matrix elements in terms of envelop functions is obtained in a way which follows "standard" $\mathbf{k}\cdot\mathbf{p}$ derivation, the only difference is the nature of microscopic integrals to be parameterized. One postulates the "slowly varying nature" of envelop functions and factors them out of the integral expression. For

example, the short-range exchange matrix element is expressed as

$$V^{\mathrm{E}}_{\mathrm{SR}}(c\sigma s, vj_z' r; c\sigma' p, vj_z q) = \sum_{i=1}^{N_{cell}} F^{s\dagger}_{c\sigma}(\mathbf{R}_i) F^{q}_{vj_z}(\mathbf{R}_i) F^{p}_{c\sigma'}(\mathbf{R}_i) F^{r\dagger}_{vj_z'}(\mathbf{R}_i) \times I_{\mathrm{SR}}(c\sigma, vj_z'; c\sigma', vj_z), \tag{11}$$

where microscopic integral

$$I_{\mathrm{SR}}(c\sigma, vj_z'; c\sigma', vj_z) = \int_{\mathbf{r}_1 \in \mathrm{WS}(\mathbf{R}_i)} \int_{\mathbf{r}_2 \in \mathrm{WS}(\mathbf{R}_i)} d\mathbf{r}_1 d\mathbf{r}_2 \times \frac{u^{\dagger}_{c\sigma}(\mathbf{r}_1) u^{\dagger}_{vj_z'}(\mathbf{r}_2) u_{c\sigma'}(\mathbf{r}_2) u_{vj_z}(\mathbf{r}_1)}{|\mathbf{r}_1 - \mathbf{r}_2|} \tag{12}$$

depends only on band labels. In the case of long-range exchange, the expression for $V^{\mathrm{E}}_{\mathrm{SR}}(c\sigma s, vj_z' r; c\sigma' p, vj_z q)$ involves the sum over $N_{cell} \times (N_{cell} - 1)$ cells and the microscopic integral is over two distinct WS cells referenced by vectors $\mathbf{R}_i$ and $\mathbf{R}_j$,

$$I_{\mathrm{LR}}(c\sigma, vj_z'; c\sigma', vj_z) = \int_{\mathbf{r}_1 \in \mathrm{WS}(\mathbf{R}_i)} \int_{\mathbf{r}_2 \in \mathrm{WS}(\mathbf{R}_j)} d\mathbf{r}_1 d\mathbf{r}_2 \times \frac{u^{\dagger}_{c\sigma}(\mathbf{r}_1) u^{\dagger}_{vj_z'}(\mathbf{r}_2) u_{c\sigma'}(\mathbf{r}_2) u_{vj_z}(\mathbf{r}_1)}{|\mathbf{r}_1 - \mathbf{r}_2|}. \tag{13}$$

Then, with the help of the truncated multipole expansion

$$1/|\mathbf{r}_1 - \mathbf{r}_2| = \frac{4\pi}{r_>} Y_{00}(\theta_1, \phi_1) Y^{\dagger}_{00}(\theta_2, \phi_2) + \frac{4\pi r_<}{3 r_>^2} \sum_{m=-1}^{1} Y_{1m}(\theta_1, \phi_1) Y^{\dagger}_{1m}(\theta_2, \phi_2),$$

$$r_< = \min(\mathbf{r}_1, \mathbf{r}_2), \quad r_> = \max(\mathbf{r}_1, \mathbf{r}_2), \tag{14}$$

one evaluates microscopic I_{SR} and I_{LR} integrals and, effectively, parameterizes the short-range and long-range exchange interactions. The higher-multipole contributions are zero due to the postulated s and p symmetries of the microscopic functions. As a result of this procedure, we obtain the following "master" expression for the exchange matrix element:

$$V^{\mathrm{E}}(c\sigma s, vj_z' r; c\sigma' p, vj_z q) = V^{\mathrm{E}}_{\mathrm{SR}}(c\sigma s, vj_z' r; c\sigma' p, vj_z q) + V^{\mathrm{E}}_{\mathrm{LR}}(c\sigma s, vj_z' r; c\sigma' p, vj_z q),$$

$$V^{\mathrm{E}}_{\mathrm{SR}}(c\sigma s, vj_z' r; c\sigma' p, vj_z q) = E_{\mathrm{SR}} (H^{int}_{\mathrm{SR}})^{c\sigma, vj_z}_{c\sigma', vj_z'} \int d\mathbf{r} F^{s\dagger}_{c\sigma}(\mathbf{r}) F^{q}_{vj_z}(\mathbf{r}) F^{p}_{c\sigma'}(\mathbf{r}) F^{r\dagger}_{vj_z'}(\mathbf{r}),$$

$$V^{\mathrm{E}}_{\mathrm{LR}}(c\sigma s, vj_z' r; c\sigma' p, vj_z q) = -\frac{4\pi}{3} \mu^2 [(\mathbf{d}^0_{c\sigma v j_z})^{\dagger} \cdot \mathbf{d}^0_{c\sigma' v j_z'}] \times \int d\mathbf{r} F^{s\dagger}_{c\sigma}(\mathbf{r}) F^{q}_{vj_z}(\mathbf{r}) F^{p}_{c\sigma'}(\mathbf{r}) F^{r\dagger}_{vj_z'}(\mathbf{r}) - \mu^2 \sum_{\gamma,\delta=1}^{3} (\mathbf{d}^0_{c\sigma v j_z})^{\dagger}_{\gamma} (\mathbf{d}^0_{c\sigma' v j_z'})_{\delta} \int \int \left[\frac{\partial^2 F^{s\dagger}_{c\sigma}(\mathbf{r}_1) F^{q}_{vj_z}(\mathbf{r}_1)}{\partial r_1^{\gamma} \partial r_1^{\delta}} \right] \times \frac{F^{p}_{c\sigma'}(\mathbf{r}_2) F^{r\dagger}_{vj_z'}(\mathbf{r}_2)}{|\mathbf{r}_1 - \mathbf{r}_2|} d\mathbf{r}_1 d\mathbf{r}_2, \tag{15}$$

where E_{SR} and μ^2 are two numerical constants parameterizing short-range and long-range exchange interactions, respectively, $(H^{int}_{\mathrm{SR}})^{c\sigma, vj_z}_{c\sigma', vj_z'}$ is an element of short-range exchange microscopic matrix,

$$\mathbf{H}^{int}_{\mathrm{SR}} = \begin{array}{c|cccc} & |c\sigma', vj_z'\rangle \left|\frac{1}{2}, -\frac{3}{2}\right\rangle & |c\sigma', vj_z'\rangle \left|\frac{1}{2}, \frac{3}{2}\right\rangle & |c\sigma', vj_z'\rangle \left|-\frac{1}{2}, -\frac{3}{2}\right\rangle & |c\sigma', vj_z'\rangle \left|-\frac{1}{2}, +\frac{3}{2}\right\rangle \\ \hline |c\sigma, vj_z\rangle \left|\frac{1}{2}, -\frac{3}{2}\right\rangle & 1 & 0 & 0 & 0 \\ |c\sigma, vj_z\rangle \left|\frac{1}{2}, +\frac{3}{2}\right\rangle & 0 & 0 & 0 & 0 \\ |c\sigma, vj_z\rangle \left|-\frac{1}{2}, -\frac{3}{2}\right\rangle & 0 & 0 & 0 & 0 \\ |c\sigma, vj_z\rangle \left|-\frac{1}{2}, +\frac{3}{2}\right\rangle & 0 & 0 & 0 & 1 \end{array} \tag{16}$$

and $\mathbf{d}^0_{c\sigma v j_z}$ are microscopic dipole elements,

$$
\begin{array}{llccc}
 & & (\mathbf{d}^0_{c\sigma v j_z})_x & (\mathbf{d}^0_{c\sigma v j_z})_y & (\mathbf{d}^0_{c\sigma v j_z})_z \\
|c\sigma, v j_z\rangle & \left|\frac{1}{2},-\frac{3}{2}\right\rangle & -1 & -i & 0 \\
|c\sigma, v j_z\rangle & \left|\frac{1}{2},+\frac{3}{2}\right\rangle & 0 & 0 & 0 \\
|c\sigma, v j_z\rangle & \left|-\frac{1}{2},-\frac{3}{2}\right\rangle & 0 & 0 & 0 \\
|c\sigma, v j_z\rangle & \left|-\frac{1}{2},+\frac{3}{2}\right\rangle & 1 & -i & 0.
\end{array}
\tag{17}
$$

The numerical parameters E_{SR} and μ^2 can be determined as to reproduce the excitonic fine structure in bulk semiconductors and, therefore, implicitly contain screening effects.

Taking into account Eqs. (16) and (17), a "block" Hamiltonian corresponding to the exchange interaction between two electron-hole pairs $F^p_c F^r_v$ and $F^s_c F^q_v$ can be presented in the form

$$
\begin{array}{llcccc}
 & & |c\sigma', v j'_z\rangle & |c\sigma', v j'_z\rangle & |c\sigma', v j'_z\rangle & |c\sigma', v j'_z\rangle \\
 & & \left|\frac{1}{2},-\frac{3}{2}\right\rangle & \left|\frac{1}{2},+\frac{3}{2}\right\rangle & \left|-\frac{1}{2},-\frac{3}{2}\right\rangle & \left|-\frac{1}{2},+\frac{3}{2}\right\rangle \\
|c\sigma, v j_z\rangle & \left|\frac{1}{2},-\frac{3}{2}\right\rangle & \delta_0^{\mathrm{SRE},L}+\delta_0^{\mathrm{LRE},L}+\delta_0^{\mathrm{LRE},N} & 0 & 0 & \delta_{12}^{\mathrm{LRE},N} \\
|c\sigma, v j_z\rangle & \left|\frac{1}{2},+\frac{3}{2}\right\rangle & 0 & 0 & 0 & 0 \\
|c\sigma, v j_z\rangle & \left|-\frac{1}{2},-\frac{3}{2}\right\rangle & 0 & 0 & 0 & 0 \\
|c\sigma, v j_z\rangle & \left|-\frac{1}{2},+\frac{3}{2}\right\rangle & \delta_{21}^{\mathrm{LRE},N} & 0 & 0 & \delta_0^{\mathrm{SRE},L}+\delta_0^{\mathrm{LRE},L}+\delta_0^{\mathrm{LRE},N}
\end{array}
\tag{18}
$$

where we separated different contributions to the exchange based on their origin (SRE or LRE) and integral type ("local" and "nonlocal"). The contributions are

$$
\delta_0^{\mathrm{SRE},L} = E_{\mathrm{SR}} \int d\mathbf{r} F_c^{s\dagger}(\mathbf{r}) F_v^q(\mathbf{r}) F_c^p(\mathbf{r}) F_v^{r\dagger}(\mathbf{r}),
$$

$$
\delta_0^{\mathrm{LRE},L} = -\frac{8\pi\mu^2}{3} \int d\mathbf{r} F_c^{s\dagger}(\mathbf{r}) F_v^q(\mathbf{r}) F_c^p(\mathbf{r}) F_v^{r\dagger}(\mathbf{r}),
$$

$$
\delta_0^{\mathrm{LRE},N} = -\mu^2 (R_{xx} + R_{yy}),
$$

$$
\begin{aligned}
\delta_{12}^{\mathrm{LRE},N} &= V_{\mathrm{LR}}^{\mathrm{E}}(1/2s, 3/2r; -1/2p, -3/2q) \\
&= \mu^2 (R_{xx} - 2iR_{xy} - R_{yy}),
\end{aligned}
$$

$$
\begin{aligned}
\delta_{21}^{\mathrm{LRE},N} &= V_{\mathrm{LR}}^{\mathrm{E}}(-1/2s, -3/2r; 1/2p, 3/2q) \\
&= \mu^2 (R_{xx} + 2iR_{xy} - R_{yy}),
\end{aligned}
$$

$$
R_{\delta\gamma} = \int\int \left\{ \left(\frac{\partial^2}{\partial r_1^\delta \partial r_1^\gamma} \right) F_c^{s\dagger} F_v^q \right\} \frac{F_c^p(\mathbf{r}_2) F_v^{r\dagger}(\mathbf{r}_2)}{|\mathbf{r}_1 - \mathbf{r}_2|} d\mathbf{r}_1 d\mathbf{r}_2. \tag{19}
$$

With regard to the above exchange expressions we note the following: (a) the short-range exchange causes splitting between bright $(|\frac{1}{2},-\frac{3}{2}\rangle, |-\frac{1}{2},+\frac{3}{2}\rangle)$ and dark doublets $(|\frac{1}{2},+\frac{3}{2}\rangle, |-\frac{1}{2},-\frac{3}{2}\rangle)$ by moving bright doublet up in energy by $\delta_0^{\mathrm{SRE},L}$. SRE does not split the bright doublet. The integral describing SRE is local in nature and involves overlap between two electron-hole pairs. (b) Long-range exchange contains expressions of two types: a local term $\delta_0^{\mathrm{LRE},L}$ which arises from $\mu^2[(\mathbf{d}^0_{c\tau v\sigma})^\dagger \cdot \mathbf{d}^0_{c\tau' v\sigma'}]$ and nonlocal terms $\delta_0^{\mathrm{LRE},N}$, $\delta_{12}^{\mathrm{LRE},N}$, and $\delta_{21}^{\mathrm{LRE},N}$ which involve differentiation operators applied to electron-hole pair envelopes. The nonlocal terms describe dipole-dipole interaction between electron-hole transition densities. (c) The splitting between bright-dark states is affected by LRE through the local LRE term $\delta_0^{\mathrm{LRE},L}$ and nonlocal LRE term $\delta_0^{\mathrm{LRE},N}$. LRE, in general, splits the bright doublet by coupling electron-hole pairs with "completely opposite" z projections of angular momentum, for example, $|-\frac{1}{2},\frac{3}{2}\rangle$ and $|\frac{1}{2},-\frac{3}{2}\rangle$. The terms which are responsible for the bright exciton splitting are $\delta_{12}^{\mathrm{LRE},N}$ and $\delta_{21}^{\mathrm{LRE},N}$—the nonlocal expressions arising from long-range exchange interaction. (d) The splitting within the dark doublet is not described in our model.

The splitting of bright exciton levels vanishes provided that $\delta_{12}^{\mathrm{LRE},N}$ and $\delta_{21}^{\mathrm{LRE},N}$ vanish which constitutes a condition

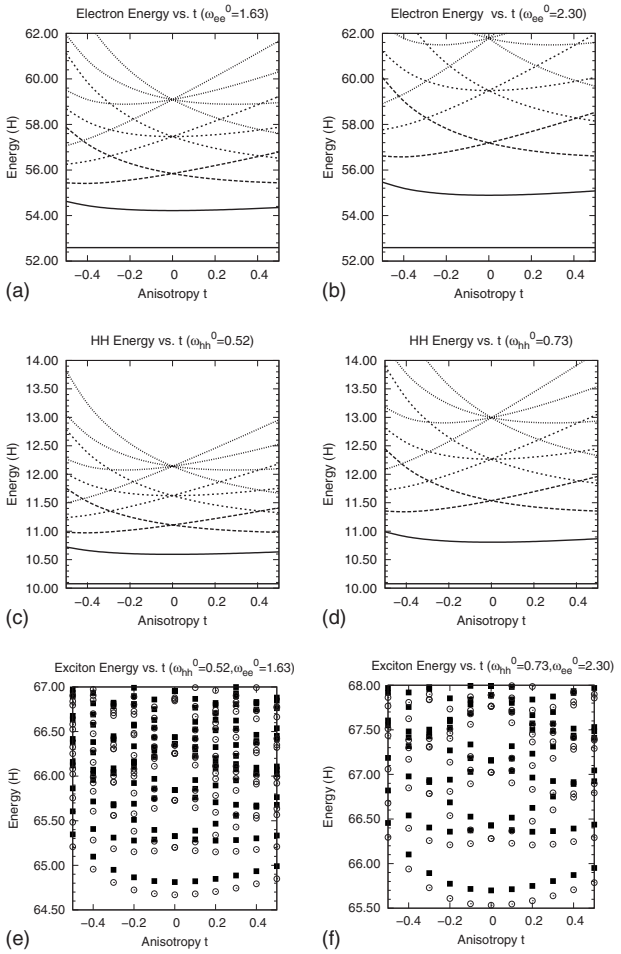

FIG. 1. Single-particle and exciton energy levels as a function of lateral anisotropy t of the confining potential.

for LRE quenching within our model. In the next section, we demonstrate numerically and analytically that this condition is fulfilled in the case of isotropic 2D HO confining potential.

III. EXCITON FINE STRUCTURE OF QUASI-2DLAHO QUANTUM DOT

In this section, we will investigate excitonic fine structure for a model quantum dot in which the confining potential is of 2D-like anisotropic harmonic-oscillator type. We note that HO spectrum has been observed in self-assembled quantum dots.[31]

The EMA equations for holes are

$$\hat{H}_{hh} = -\frac{1}{2M_{\parallel,hh}}(\nabla_x^2 + \nabla_y^2) + \frac{1}{2}M_{\parallel,hh}(\omega_{x,hh}^2 x^2 + \omega_{y,hh}^2 y^2) - \frac{1}{2M_{\perp,hh}}\nabla_z^2 + \frac{1}{2}M_{\perp,hh}\omega_{z,hh}^2 z^2,$$

$$\omega_{x,hh} = \omega_{hh}^0(1+t), \quad \omega_{y,hh} = \frac{\omega_{hh}^0}{1+t}, \quad \omega_{x,hh}\omega_{y,hh} = (\omega_{hh}^0)^2 = \text{const}, \quad \omega_{z,hh} \gg \omega_{hh}^0, \tag{20}$$

where $M_{\parallel,hh}$ and $M_{\perp,hh}$ are effective masses, $\omega_\gamma(\gamma=x,y,z)$ denotes confinement frequency in x, y, and z directions, respectively, ω_{hh}^0 determines the typical energy scale of the confining potential and, together with the mass and the confinement. The energies and lengths are expressed in the effective units.

EMA equations for electrons have a similar form

$$\hat{H}_{ee} = -\frac{1}{2}(\nabla_x^2 + \nabla_y^2 + \nabla_z^2) + \frac{1}{2}(\omega_{x,ee}^2 x^2 + \omega_{y,ee}^2 y^2 + \omega_{z,ee}^2 z^2),$$

$$\omega_{x,ee} = \omega_{ee}^0(1+t), \quad \omega_{y,ee} = \frac{\omega_{ee}^0}{1+t}, \quad \omega_{x,ee}\omega_{y,ee} = (\omega_{ee}^0)^2 = \text{const}, \quad \omega_{z,ee} \gg \omega_{ee}^0. \tag{21}$$

The excitonic fine structure is studied as a function of anisotropy t. For example, for $t=-0.5$, $\omega_x=(1/2)\omega^0$, and $\omega_y=2\omega^0$, the confinement along x is weaker than along y. For $t=0.5$, $\omega_x=(3/2)\omega^0$, and $\omega_y=2/3\omega^0$, confinement along x is greater than along y. In the case $t=0$, the confining potential for holes and electrons is isotropic in the lateral direction. By changing anisotropy t, we control the shape of the confining potentials for holes [Eq. (20)] and electrons [Eq. (21)] and, as a consequence, the single-particle energy spectra and eigenfunctions.

We have assumed that the confinement in the vertical direction z is much stronger than confinement in the lateral direction $\omega_z \gg \omega^0$. Therefore, we will always assume the ground-state solution in z direction and the single-particle energy spectra for holes [Eq. (20)] and electrons [Eq. (21)] is 2D like,

$$E(n,m,0) = \left(n+\frac{1}{2}\right)\omega_x + \left(m+\frac{1}{2}\right)\omega_y + \frac{1}{2}\omega_z, \tag{22}$$

where n and m are 2DLAHO quantum numbers. In what follows, we use numerical parameters $M_{\parallel,hh}=9.930853$, $M_{\perp,hh}=5.218662$, $M_{\parallel,ee}=1.0$, $M_{\perp,ee}=1.0$, $\omega_{z,hh}=20.155737$, and $\omega_{z,ee}=105.185977$.

The eigenfunctions are products of one-dimensional Hermite polynomials and exponential function,

$$\psi_{nm0}(\mathbf{r}) = \psi_n(x)\psi_m(y)\psi_0(z), \tag{23}$$

where the eigenfunction in one of the Cartesian directions (for example, x) is given by

$$\psi_n(x) = \sqrt{\frac{1}{2^n n!}}\left(\frac{m\omega_x}{\pi}\right)^{1/4}\exp\left(-\frac{m\omega_x}{2}x^2\right)H_n(\sqrt{m\omega_x}x),$$

$$H_n(x) = (-1)^n\exp(x^2)\frac{d^n}{dx^n}\exp(-x^2). \tag{24}$$

Figures 1(a)–1(d) show single-particle spectra for electrons and holes, respectively, for two different characteristic energy scales ω^0. Solid horizontal line (around 52.6 and 10.1 hartree for electrons and holes, respectively) corresponds to the confinement energy in vertical direction $\omega_z/2$.

The single-particle energy spectra are given by Eq. (22). The single-particle ground state is the nodeless s envelope which corresponds to $n=m=0$. The "excited" levels are or-

ganized in shells referred to as p, d, f, and so on with characteristic "spatial" degeneracies of 2, 3, 4, etc., in the case of isotropic ($t=0$) confinement potential. The dispersion $E(t)$ of s energy level with anisotropy is weak compared to the dispersion of excited envelopes. Strong anisotropy might lead to the level crossing where the single-particle energy of d-type envelope is below the single-particle energy of p-type envelope. The level crossing happens, for example, at $t\approx -0.3$ for the second excited state in Fig. 1(a). Due to the smaller effective mass of electrons, the spacing between electron single-particle levels is larger than that of the hole levels.

Figures 1(e) and 1(f) show "noninteracting" electron-hole and "interacting" exciton energies as a function of lateral anisotropy t for two different characteristic energy scales ω^0. The black squares in Figs. 1(e) and 1(f) correspond to the noninteracting electron-hole pair energies $\delta_{v\sigma q,v\sigma' r}\delta_{c\tau s,c\tau' p}(\varepsilon^h_{v\sigma q}+\varepsilon^e_{c\tau s})$. The empty circles are obtained by diagonalizing the full excitonic Hamiltonian. Each of the empty circles is actually a multiplet of four exciton states with fine structure determined by the electron-hole exchange interaction. The noninteracting electron-hole and excitonic spectra look quite similar. The Coulomb electron-hole attraction simply decreases the exciton energy. The Coulomb attraction-induced mixing of electron-hole pairs in an exciton is small due to the large separation of single-particle levels compared with the magnitude of screened Coulomb attraction.

In the lower part of the interacting excitonic energy spectra and for small anisotropies $|t|\leq 0.2$, the dispersion $E_X(t)$ strongly resembles that of the dispersion of single-particle levels. This happens because $\omega^0_{hh}<\omega^0_{ee}$ and the lowest-energy electron-hole pairs follow the order of hole levels $s_e s_h$, $s_e p_h$, and $s_e d_h$.

A. LRE interaction for s-type envelopes

Consider the case when exciton is given by the product of ground-state envelopes of electron and hole single-particle states ($s_e s_h$ exciton). In this case,

$$F_c^\dagger(\mathbf{r})F_v(\mathbf{r}) = N_c N_v \exp(-\alpha_x x^2 - \alpha_y y^2 - \alpha_z z^2),$$

$$N_c = \left(\frac{2\alpha_{xc}}{\pi}\right)^{1/4}\left(\frac{2\alpha_{yc}}{\pi}\right)^{1/4}\left(\frac{2\alpha_{zc}}{\pi}\right)^{1/4},$$

$$N_v = \left(\frac{2\alpha_{xv}}{\pi}\right)^{1/4}\left(\frac{2\alpha_{yv}}{\pi}\right)^{1/4}\left(\frac{2\alpha_{zv}}{\pi}\right)^{1/4},$$

$$\alpha_x = \alpha_{xc} + \alpha_{xv}, \quad \alpha_y = \alpha_{yc} + \alpha_{yv}, \quad \alpha_z = \alpha_{zc} + \alpha_{zv},$$

$$\alpha_{xc} = \frac{\omega_{x,ee}}{2}, \quad \alpha_{yc} = \frac{\omega_{y,ee}}{2}, \quad \alpha_{zc} = \frac{\omega_{z,ee}}{2},$$

$$\alpha_{xv} = \frac{M_{\parallel,hh}\omega_{x,hh}}{2}, \quad \alpha_{yv} = \frac{M_{\parallel,hh}\omega_{y,hh}}{2}, \quad \alpha_{zv} = \frac{M_{\perp,hh}\omega_{z,hh}}{2}, \tag{25}$$

where N_c and N_v are normalization constants, $\alpha_{\gamma c}$ and $\alpha_{\gamma v}(\gamma=x,y,z)$ denote confinements of electrons and holes in x, y, and z directions, respectively, and $\alpha_\gamma=\alpha_{\gamma c}+\alpha_{\gamma v}$ denote confinements of electron-hole envelope.

The matrix elements responsible for bright exciton splitting for $s_e s_h$ exciton are given by

$$\delta_{12}^{\mathrm{LRE},N} = \mu^2(R_{xx} - 2iR_{xy} - R_{yy}),$$

$$\delta_{21}^{\mathrm{LRE},N} = \mu^2(R_{xx} + 2iR_{xy} - R_{yy}), \tag{26}$$

where

$$R_{xx} = \int\int \left(\frac{\partial^2 F_c^\dagger F_v}{\partial x_1^2}\right)\frac{F_c(\mathbf{r}_2)F_v^\dagger(\mathbf{r}_2)}{|\mathbf{r}_1-\mathbf{r}_2|}d\mathbf{r}_1 d\mathbf{r}_2 = -\frac{(N_c N_v)^2}{\alpha_x\alpha_y\alpha_z}\pi\sqrt{\pi}I_x(\alpha_x,\alpha_y,\alpha_z),$$

$$I_x(\alpha_x,\alpha_y,\alpha_z) = \int_0^{\pi/2}\int_0^{\pi/2}\frac{\sin^3\theta\cos^2\phi d\theta d\phi}{\left[\sin^2\theta\left(\frac{1}{2\alpha_x}\cos^2\phi + \frac{1}{2\alpha_y}\sin^2\phi\right) + \frac{1}{2\alpha_z}\cos^2\theta\right]^{3/2}},$$

$$R_{yy} = \int\int \left(\frac{\partial^2 F_c^\dagger F_v}{\partial y_1^2}\right)\frac{F_c(\mathbf{r}_2)F_v^\dagger(\mathbf{r}_2)}{|\mathbf{r}_1-\mathbf{r}_2|}d\mathbf{r}_1 d\mathbf{r}_2 = -\frac{(N_c N_v)^2}{\alpha_x\alpha_y\alpha_z}\pi\sqrt{\pi}I_y(\alpha_x,\alpha_y,\alpha_z),$$

$$I_y(\alpha_x,\alpha_y,\alpha_z) = \int_0^{\pi/2}\int_0^{\pi/2}\frac{\sin^3\theta\sin^2\phi d\theta d\phi}{\left[\sin^2\theta\left(\frac{1}{2\alpha_x}\cos^2\phi + \frac{1}{2\alpha_y}\sin^2\phi\right) + \frac{1}{2\alpha_z}\cos^2\theta\right]^{3/2}},$$

$$R_{xy} = \int\int \left(\frac{\partial^2 F_c^\dagger F_v}{\partial y_1\,\partial x_1}\right)\frac{F_c(\mathbf{r}_2)F_v^\dagger(\mathbf{r}_2)}{|\mathbf{r}_1-\mathbf{r}_2|}d\mathbf{r}_1 d\mathbf{r}_2 = 0. \tag{27}$$

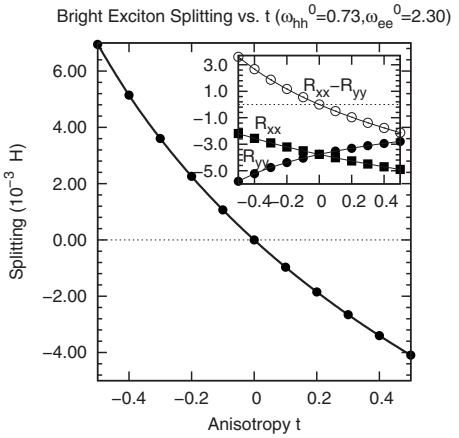

FIG. 2. Bright exciton doublet splitting as a function of lateral anisotropy t of the confining potential. Inset: R_{xx} (dark squares) and R_{yy} (dark circles) contributions to nonlocal LRE matrix elements as a function of anisotropy of the confining potential; $R_{xx}-R_{yy}$ (empty circles) difference of two nonlocal LRE contributions that determines the bright exciton splitting. For the isotropic confining potential $t=0$ and $R_{xx}-R_{yy}=0$.

It follows from Eq. (27) that $\delta_{12}^{\mathrm{LRE},N}$ and $\delta_{21}^{\mathrm{LRE},N}$ vanish provided that the "confinement" of electron-hole pair envelope is identical in x and y directions ($\alpha_x=\alpha_y$). Figure 2 illustrates this. Figure 2 shows bright exciton doublet splitting as a function of lateral anisotropy t. The doublet splitting energy is defined as $E_X^y-E_X^x$, where E_X^x and E_X^y are ground-state bright exciton energy levels polarized along x and y directions, respectively. For $t<0(\omega_x<\omega_y)$, $E_X^y>E_X^x$ and the bright ground state is dipole active along the x axis whereas for $t>0(\omega_x<\omega_y)$ the bright ground state is dipole active along the y axis. In our model, the bright ground state is always dipole active along the axis of weaker confinement. The inset of Fig. 2 shows R_{xx} and R_{yy} nonlocal contributions to LRE exchange as a function of anisotropy computed from Eq. (27). We can see that R_{xx} increases and R_{yy} decreases in magnitude as t goes from −0.5 to 0.5. The inset also shows the difference $R_{xx}-R_{yy}$ which determines bright exciton splitting as a function of anisotropy. We can see that $R_{xx}-R_{yy}$ steadily decreases as a function of t and passes through zero at $t=0$. $t=0$ corresponds to the laterally isotropic confining potential. In this case, $R_{yy}=R_{xx}$ and the exchange matrix element which couple two bright exciton levels vanishes. As a result, the splitting between bright excitons vanishes as well. We note, once again, that this result is obtained assuming rotational symmetry $C_{\infty v}$ of the confining potential as well the dipole-dipole nature of the LRE interaction which stems from orthogonality of the electron and hole functions on the unit-cell scale in bulk.

B. Application of lateral electric field

In the previous section, we have demonstrated that the magnitude of the bright exciton exchange splitting can be controlled through the shape of the confining potential. In practice, one may, for example, try to quench the bright exciton splitting by picking "symmetric" dots from a large number of samples grown under different conditions.[6] Nevertheless, the growth of QD is essentially a random process and control through the QD shape is hard to achieve.

It is, therefore, of great interest to examine the effects of external fields on the excitonic fine structure. For example, QDs can be placed[2] between Schottky gates for the application of vertical and lateral electric fields. Recently, it has been demonstrated theoretically[32] and experimentally[13] that by applying an in-plane electric field it is possible to fine-tune photon cascades originating from recombination of multiexciton complexes in QDs.

The electron-hole exchange interaction was treated in Ref. 32 using empirical exchange Hamiltonian. This section discusses the effects of the lateral electric field on the exchange matrix elements of our effective EMA Hamiltonian (18). We will focus on the bright exciton splitting as a function of the lateral electric field.

Within our model, application of lateral electric field $\vec{F}=F\mathbf{e}_x+F\mathbf{e}_y$ of magnitude $|F|$ displaces the "origin" of electron and hole envelopes in xy plane from (0,0) to (x_0^e,y_0^e) and (x_0^h,y_0^h), respectively. The single-particle energy levels are rigidly shifted by the Stark shift whereas the spacing between the single-particle energy levels of HO is not affected. The "separation" of electron and hole envelopes in xy plane is determined by equations

$$\Delta x_0 = x_0^e - x_0^h = eF\left(\frac{1}{\omega_{x,ee}^2}+\frac{1}{M_{\parallel,hh}\omega_{x,hh}^2}\right),$$

$$\Delta y_0 = y_0^e - y_0^h = eF\left(\frac{1}{\omega_{y,ee}^2}+\frac{1}{M_{\parallel,hh}\omega_{y,hh}^2}\right). \tag{28}$$

Evaluating the integrals which control bright exciton splitting $R_{xx}(F)$, $R_{yy}(F)$, and $R_{xy}(F)$ as a function of field F for $s_e s_h$ electron-hole envelope, we obtain

$$R_{xx}(F) = R_{xx}(0)\exp\left(-\frac{2\alpha_{xc}\alpha_{xv}}{\alpha_x}\Delta x_0^2-\frac{2\alpha_{yc}\alpha_{yv}}{\alpha_y}\Delta y_0^2\right),$$

$$R_{yy}(F) = R_{yy}(0)\exp\left(-\frac{2\alpha_{xc}\alpha_{xv}}{\alpha_x}\Delta x_0^2-\frac{2\alpha_{yc}\alpha_{yv}}{\alpha_y}\Delta y_0^2\right),$$

$$R_{xy}(F) = 0, \tag{29}$$

where $R_{xx}(0)$ and $R_{yy}(0)$ are integrals [Eq. (27)] in the absence of the electric field ($F=0$). Field dependence of $R_{xx}(F)-R_{yy}(F)$ which determines the bright exciton splitting is shown in Fig. 3 for five different initial values of lateral anisotropy. At $F=0$, the bright exciton splitting attains maximum value which is determined by the initial shape anisotropy of the confining potential. The larger the magnitude of the anisotropy, the larger is the initial ($F=0$) bright exciton splitting. As F increases in magnitude, the electron and hole envelopes are pulled out in opposite direction and the magnitude of the splitting is reduced. Since the separation between the envelopes depends on F^2, the splitting is independent of the sign of the field F.

It is interesting to note that the "rate of quenching" of the splitting depends on the initial anisotropy—the stronger the

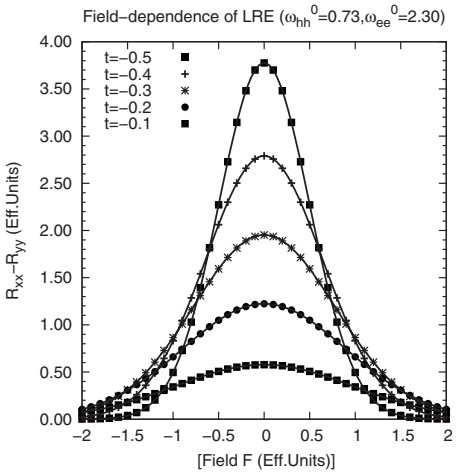

FIG. 3. Nonlocal LRE $R_{xx}-R_{yy}$ which determines bright exciton splitting as a function of lateral electric field F. At $F=0$, $R_{xx}-R_{yy}$ attains maximum determined by the initial anisotropy of the confining potential. As magnitude of field F increases, $R_{xx}-R_{yy}$ decreases due to the separation of electron and hole envelopes.

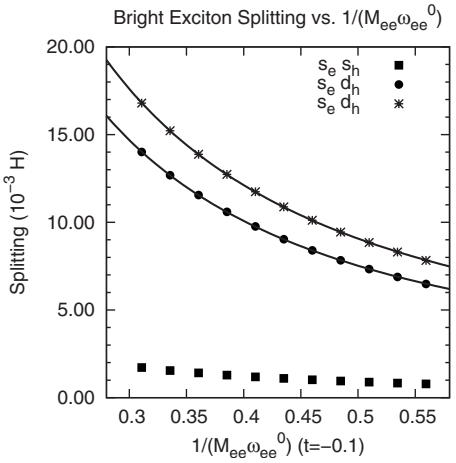

FIG. 4. Size scaling of the bright exciton doublet splittings. Lateral anisotropy is kept constant $t=-0.1$. The doublet splittings are plotted as a function of $1/(M_{\|,ee}\omega_{ee}^0)$. The ratio $\omega_{ee}^0/\omega_{hh}^0$ is kept constant. The ground exciton is of s_e-s_h type. Two excited bright excitons correspond to s_e-d_h electron-hole pairs. The solid lines are fit to the power law C/R^n, where C is a constant, $n\approx 1.30$.

confinement, the larger is the drop in the magnitude of the splitting. One can use lateral electric field to produce two identical bright exciton splittings for two dots with different initial anisotropies. This happens, for example, at $|F|\approx 0.6$ for two dots with initial anisotropies of $t=-0.5$ and $t=-0.4$, respectively.

C. Scaling of bright exciton splitting

The question of size scaling of exchange interactions in nanosystems has received a lot of attention, particularly, in connection with the Stokes ("red") shift of resonant PL spectra with respect to the absorption edge (see, for example, Ref. 19). In this section, we examine the size scaling of bright exciton splitting as a function of system's size.

Suppose that R is a characteristic size of a 2D-like system. From the normalization condition

$$\int d\mathbf{r}|F_c(\mathbf{r})|^2=1, \quad \int d\mathbf{r}|F_v(\mathbf{r})|^2=1, \tag{30}$$

envelope functions scale as $1/R^2$. Based on this "normalization" argument, the nonlocal LRE integrals R_{xx}, R_{yy}, and R_{xy} that determine bright exciton splitting scale as

$$\frac{1}{R^2}\frac{1}{R^2}\frac{1}{R}\frac{1}{R^2}R^2R^2\propto\frac{1}{R^3}. \tag{31}$$

The dependence [Eq. (31)] is expected to hold in the strong confinement regime. Of course, one has to keep in mind that the exchange matrix element responsible for the bright exciton splitting is a linear combination of nonlocal LRE integrals R_{xx}, R_{yy}, and R_{xy}. Therefore, the actual size dependence of bright exciton splitting might be different from $1/R^3$ and depend strongly on the "nature" of the envelope functions involved in the LRE integrals.

We will examine the bright exciton splitting as a function of the confinement length squared $l^2=1/(M_{\|}\omega^0)$. The ratio of electron and hole confinement frequencies is kept constant $\omega_{ee}^0/\omega_{hh}^0$=const and the lateral anisotropy t is fixed. Since $\omega_{ee}^0/\omega_{hh}^0$=const, by increasing/decreasing ω_{ee}^0 we automatically increasing/decreasing ω_{hh}^0.

Figure 4 shows the scaling of the splittings for the ground and excited bright exciton levels with size. The lateral anisotropy is fixed to $t=-0.1$ in all the calculations. We find that splittings decay as the size of the system increases. We find that the ground-state exciton splitting is size insensitive whereas the splittings of the excited bright excitons scale $\propto 1/R^{1.3}$. This scaling is different from $1/R^3$ dependence expected from the normalization arguments [Eq. (31)]. The deviation might be due to the fact that the exchange matrix elements that determine the bright exciton splitting δ_{12} and δ_{21} involve a linear combination of nonlocal exchange integrals R_{xx}, R_{yy}, and R_{xy}. Moreover, R_{xx} and R_{yy} enter the expression for δ_{12} and δ_{21} with different sign and some cancellation of terms may occur. Therefore, the size dependence of bright exciton splittings may depend strongly on the details of the excitonic wave function.

IV. CONCLUSIONS

A four-band electron-hole excitonic Hamiltonian is derived within the EMA which takes into account the electron-hole exchange interaction. The matrix elements of the effective Hamiltonian are expressed explicitly in terms of electron and hole envelopes. The microscopic parts of single-particle orbitals are integrated out and enter our Hamiltonian implicitly through numerical parameters. The matrix element responsible for the bright exciton splitting is identified and analyzed. An explicit expression for this matrix element in terms of electron and hole envelopes is presented. An excitonic fine structure for a model system with 2D-like aniso-

tropic HO confining potential is considered. It is found that in the case of 2D isotropic potential, the bright exciton splitting vanishes. Within the formalism of our effective excitonic Hamiltonian, the effects of the lateral electric field on the excitonic fine structure were considered. It is found that the excitonic structure can be tuned with lateral electric field and that the magnitude of the exchange splitting is reduced. The origin of this reduction is the spatial separation of electron-hole pairs by electric field. Finally, size dependence of the bright exciton splittings for the ground- and excited-state excitons was investigated and it was found that the size scaling of bright exciton splitting can be different from the laws established using normalization conditions.

ACKNOWLEDGMENTS

The authors acknowledge discussions with M. Korkusinki, M. Zielinski, R. Williams, and D. Dalacu and support by the NRC-NSERC-BDC Nanotechnology project, QuantumWorks, NRC-CNRS CRP, and CIFAR. The authors thank E. L. Ivchenko for reading the manuscript and making useful suggestions.

*ekadants@babylon.phy.nrc.ca

[1] O. Benson, C. Santori, M. Pelton, and Y. Yamamoto, Phys. Rev. Lett. **84**, 2513 (2000).
[2] D. Dalacu, S. Frederick, D. Kim, M. E. Reimer, J. Lapointe, P. J. Poole, G. C. Aers, R. L. Williams, W. R. McKinnon, M. Korkusinski, and P. Hawrylak, Laser Photonics Rev. (to be published).
[3] L. Jacak, P. Hawrylak, and A. Wojs, *Quantum Dots* (Springer-Verlag, Berlin, 1998).
[4] P. Hawrylak and M. Korkusinski, *Single Quantum Dots: Fundamentals, Applications, and New Concepts*, Topics in Applied Physics Vol. 90 (Springer-Verlag, Berlin, 2003).
[5] A. J. Shields, Nat. Photonics **1**, 215 (2007).
[6] R. M. Stevenson, R. J. Young, P. Atkinson, K. Cooper, D. A. Ritchie, and A. J. Shields, Nature (London) **439**, 179 (2006).
[7] N. Akopian, N. H. Lindner, E. Poem, Y. Berlatzky, J. Avron, D. Gershoni, B. D. Gerardot, and P. M. Petroff, Phys. Rev. Lett. **96**, 130501 (2006).
[8] A. Greilich, M. Schwab, T. Berstermann, T. Auer, R. Oulton, D. R. Yakovlev, M. Bayer, V. Stavarache, D. Reuter, and A. Wieck, Phys. Rev. B **73**, 045323 (2006).
[9] M. Bayer, G. Ortner, O. Stern, A. Kuther, A. A. Gorbunov, A. Forchel, P. Hawrylak, S. Fafard, K. Hinzer, T. L. Reinecke, S. N. Walck, J. P. Reithmaier, F. Klopf, and F. Schäfer, Phys. Rev. B **65**, 195315 (2002).
[10] M. Bayer, A. Kuther, A. Forchel, A. Gorbunov, V. B. Timofeev, F. Schäfer, J. P. Reithmaier, T. L. Reinecke, and S. N. Walck, Phys. Rev. Lett. **82**, 1748 (1999).
[11] K. Kowalik, O. Krebs, A. Lemaitre, S. Laurent, P. Senellart, P. Voisin, and J. A. Gaj, Appl. Phys. Lett. **86**, 041907 (2005).
[12] M. M. Vogel, S. M. Ulrich, R. Hafenbrak, P. Michler, L. Wang, A. Rastelli, and O. G. Schmidt, Appl. Phys. Lett. **91**, 051904 (2007).
[13] M. E. Reimer, M. Korkusinski, D. Dalacu, J. Lefebvre, J. Lapointe, P. J. Poole, G. C. Aers, W. R. McKinnon, P. Hawrylak, and R. L. Williams, Phys. Rev. B **78**, 195301 (2008).
[14] R. S. Knox, *Solid State Phys.* (Academic, New York, 1963), Vol. 5.
[15] M. M. Denisov and V. P. Makarov, Phys. Status Solidi B **56**, 9 (1973).
[16] G. L. Bir and G. E. Pikus, *Simmetriya i deformatsionnye effekty v poluprovodnikakh* (Nauka, Moscow, 1972).
[17] T. Takagahara, Phys. Rev. B **47**, 4569 (1993).
[18] M. Z. Maialle, E. A. de Andrada e Silva, and L. J. Sham, Phys. Rev. B **47**, 15776 (1993).
[19] A. L. Efros, M. Rosen, M. Kuno, M. Nirmal, D. J. Norris, and M. Bawendi, Phys. Rev. B **54**, 4843 (1996).
[20] S. V. Gupalov, E. L. Ivchenko, and A. V. Kavokin, J. Exp. Theor. Phys. **86**, 388 (1998).
[21] T. Takagahara, Phys. Rev. B **62**, 16840 (2000).
[22] S. V. Gupalov and E. L. Ivchenko, Phys. Solid State **42**, 2030 (2000).
[23] M. M. Glazov, E. L. Ivchenko, L. Besombes, Y. Leger, L. Maingault, and H. Mariette, Phys. Rev. B **75**, 205313 (2007).
[24] A. Franceschetti, L. W. Wang, H. Fu, and A. Zunger, Phys. Rev. B **58**, R13367 (1998).
[25] S. V. Goupalov and E. L. Ivchenko, Phys. Solid State **43**, 1867 (2001).
[26] G. Bester, S. Nair, and A. Zunger, Phys. Rev. B **67**, 161306(R) (2003).
[27] L. He, M. Gong, C.-F. Li, G.-C. Guo, and A. Zunger, Phys. Rev. Lett. **101**, 157405 (2008).
[28] M. Korkusinski, M. Zielinski, and P. Hawrylak, J. Appl. Phys. **105**, 122406 (2009).
[29] E. L. Ivchenko, *Optical Spectroscopy of Semiconductor Nanostructures* (Alpha Science International, Harrow, UK, 2005).
[30] A. Wojs, P. Hawrylak, S. Fafard, and L. Jacak, Phys. Rev. B **54**, 5604 (1996).
[31] S. Raymond, S. Studenikin, A. Sachrajda, Z. Wasilewski, S. J. Cheng, W. Sheng, P. Hawrylak, A. Babinski, M. Potemski, G. Ortner, and M. Bayer, Phys. Rev. Lett. **92**, 187402 (2004).
[32] M. Korkusinski, M. E. Reimer, R. L. Williams, and P. Hawrylak, Phys. Rev. B **79**, 035309 (2009).